J. Biochem. 128, 1059–1072 (2000)

Identification of a Cryptic N-Terminal Signal in *Saccharomyces cerevisiae* Peroxisomal Citrate Synthase That Functions in Both Peroxisomal and Mitochondrial Targeting[1]

Jeong Goo Lee,[*] Seong Pil Cho,[*,2] Heon Sik Lee,[*] Cheong Ho Lee,[†] Kyung Sook Bae,[‡] and Pil Jae Maeng[*,3]

[*] *Department of Microbiology, Chungnam National University, Yusong-Gu, Taejon 305-764, Korea;* [†]*Ginseng and Tobacco Research Institute, Yusong-Gu, Taejon 305-345, Korea; and* [‡]*Culture Collection Program, Genetic Resources Center, KRIBB, Yusong-Gu, Taejon 305-606, Korea*

Received August 29, 2000; accepted October 4, 2000

***Saccharomyces cerevisiae* has three distinct citrate synthases, two located in mitochondria (mature Cit1p and Cit3p) and one in peroxisomes (mature Cit2p). While the precursor of the major mitochondrial enzyme, Cit1p, has a signal for mitochondrial targeting at its N-terminus (MTS), Cit2p has one for peroxisomal targeting (PTS1) at its C-terminus. We have previously shown that the N-terminal segment of Cit2p is removed during import into peroxisomes [Lee, H.S. *et al.* (1994) *Kor. J. Microbiol.* 32, 558–564], which implied the presence of an additional N-terminal sorting signal. To analyze the function of the N-terminal region of Cit2p in protein trafficking, we constructed the N-terminal domain–swapped versions of Cit1p and Cit2p. Both fusions, Cit1::Cit2 and Cit2::Cit1, complemented the glutamate auxotrophy caused by the double-disruption of the *CIT1* and *CIT2* genes. In addition, part of the Cit2::Cit1 fusion protein, as well as Cit1::Cit2, was shown to be transported into both mitochondria and peroxisomes. The subcellular localization of the recombinant fusion proteins containing various N-terminal segments of Cit2p fused to a mutant version of green fluorescent protein (GFP2) was also examined. As a result, we found that the 20-amino acid N-terminal segment of Cit2p contains a cryptic cleavable targeting signal for both peroxisomes and mitochondria. In addition, we show that the peroxisomal import process mediated by the N-terminal segment of Cit2p was not affected by the disruption of either *PEX5* (encoding PTS1 receptor) or *PEX7* (encoding PTS2 receptor).**

Key words: citrate synthase, mitochondria, peroxisomes, *Saccharomyces cerevisiae*, targeting signal.

In eukaryotic cells, mitochondria and peroxisomes share a variety of enzymatic reactions. For example, the TCA cycle occurring in mitochondria and the related glyoxylate cycle taking place in peroxisomes have many reactions in common. Thus the two organelles contain isozymes catalyzing these related reactions.

Most mitochondrial proteins are synthesized in the cytoplasm as larger precursors and are imported into the mitochondria. The precursors of mitochondrial proteins contain N-terminal mitochondrial targeting signals (MTSs) that mediate their import into mitochondria and are then removed by one or two proteolytic steps (*1*, *2*). Peroxisomal proteins are also synthesized in the cytosol and transported into peroxisomes. Three types of peroxisomal targeting signals (PTSs) have been described. PTS1, which is used by the vast majority of peroxisomal proteins including firefly luciferase (*3*), rat urate oxidase (*4*), and rat acyl-CoA oxidase (*5*), consists of a C-terminal tripeptide SKL (serine-lysine-leucine) or closely related variants, and is not cleaved off in the peroxisomal import process. PTS2 is contained within the N-terminal region of selected peroxisomal proteins, such as peroxisomal 3-oxoacyl-CoA thiolases of *Saccharomyces cerevisiae* (*6*, *7*), cucumber (*8*), and rat (*9*, *10*), watermelon glyoxisomal malate dehydrogenase (*11*), and *Hansenula polymorpha* amine oxidase (*12*, *13*). The third type of PTS is located in internal protein sequences, such as those found in *Candida tropicalis* acyl-CoA oxidase (*14*) and *S. cerevisiae* catalase A (*15*).

S. cerevisiae has three distinct citrate synthases [EC 4.1.3.7] that catalyze the formation of citrate from acetyl-CoA and oxaloacetate. The mature form of Cit1p is the major mitochondrial citrate synthase and functions as the rate-limiting enzyme in the TCA cycle (*16*). Mature Cit2p is the peroxisomal enzyme and is involved in the biosynthesis of glutamate and/or the glyoxylate cycle (*17–19*). Cit3p is the precursor of a minor mitochondrial form and is poorly expressed under normal growth conditions (*20*). Among the citrate synthase precursors, Cit1p and Cit2p share a high

[1] This work was supported by Non-Directed Research Fund (Project No. 01-D-0311), Korea Research Foundation, 1996.

[2] Present Address: Mogam Biotechnology Research Institute, Yongin, Kyunggi 449-910, Korea.

[3] To whom correspondence should be addressed. Tel: +82-42-821-6415, Fax: +82-42-822-7367, E-mail: pjmaeng@cnu.ac.kr

Abbreviations: GFP, green fluorescent protein; PTS, peroxisomal targeting signal; MTS, mitochondrial targeting signal.

© 2000 by the Japanese Biochemical Society.

Downloaded from http://jb.oxfordjournals.org/ at Peking University on October 1, 2012

degree of similarity with each other (81%) (*20*). The N-terminal regions of Cit1p and Cit2p share significant similarity with those of *Escherichia coli* and porcine citrate synthases; however, sequences that extend beyond these related N-terminal segments are strikingly divergent (*19*).

In our previous studies, we have found that the N-terminal 37 amino acids of Cit1p are removed in the process of mitochondrial targeting by proteolytic cleavage at the R-3 motif ($R_{(35)}$-H-Y↓$S_{(38)}$). Furthermore, we showed that although Cit2p has a C-terminal PTS1, the N-terminal segment of Cit2p is also removed during import into peroxisomes (*21, 22*). This result implies presence of an additional sorting signal in the N-terminal segment of Cit2p.

In the present study, we sought to determine the function of the N-terminal region of Cit2p in the process of intracellular protein sorting. We constructed N-terminal domain–swapped citrate synthases and various fusions of GFP2 (GFP with Ser 65→Thr mutation) (*23*) containing variable lengths of the Cit2p N-terminal segment. Here we present evidence indicating that the N-terminal segment of Cit2p is capable of functioning as a signal for targeting proteins to both mitochondria and peroxisomes.

MATERIALS AND METHODS

Strains, Media, and Transformation—*S. cerevisiae* strains were grown on either YPD (complete medium), YEP (same as YPD, except that 20 g/liter of glucose was replaced by 20 g/liter of the carbon source indicated), or YNB (minimal medium supplemented with 100 mg/liter of lysine) (*21*). Transformation of *S. cerevisiae* strains was performed using the lithium acetate method (*24*). The *S. cerevisiae* strains used in this study are listed in Table I. *S. cerevisiae* MPY001 (*cit1::LEU2 cit2::ura3-508 leu2 ura3*) was derived from PSY44 (*cit1::LEU2 cit2::URA3 leu2 ura3*) as follows. The *URA3* gene contained in YEp352 (*25*) was cut at the unique *Nco*I site. The resulting *Nco*I ends of the plasmid were filled in with Klenow enzyme (Promega, Madison, Wisconsin, USA) and self-ligated to yield a mutant allele, *ura3-508*. After transformation of PSY44 with the ligated DNA, mutants harboring *ura3-508* (instead of *URA3*) were selected on YNB supplemented with 1 g/liter of 5-fluoroorotic acid, 100 mg/liter of uridine, 100 mg/liter of lysine, and 200 mg/liter of glutamate.

E. coli DH5α cells were grown in Luria-Bertani (LB) medium and transformed by standard methods (*26*).

Construction of Plasmids—The plasmids used in this study are listed in Table I. For the construction of chimeric genes encoding the N-terminal domain–swapped citrate synthases, segments of *CIT1* and *CIT2* were amplified by PCR using pLCS1 and pUCS2 (*21*) as templates. These vectors were derived from YEp351 and YEp352 (*25*) by insertion of the 2.7-kb *Sma*I–*Pst*I *CIT1* fragment (*16*) and 2.1-kb *Eco*RI *CIT2* fragment (*17*), respectively.

The hybrid gene for the Cit1::Cit2 protein containing the 85–amino acid N-terminal segment of Cit1p fused to the 392–amino acid C-terminal segment of Cit2p, was constructed as follows. First, the 1.6-kb *cit2* fragment coding for the C-terminal segment of Cit2p was amplified by PCR from pUCS2 using primers P4 (5′TGGTATGAGAGGAATTCCAGGGAGCGTATG3′) and P2 (5′CCAAGCTTGCATGCCTGCAG3′) (Fig. 1). PCR was performed with a DNA thermal cycler (GeneAmp PCR system 2400; Perkin-Elmer Cetus, Norwalk, Connecticut, USA) using *Taq* DNA polymerase (Boehringer Mannheim, Mannheim, Germany). After digestion with *Eco*RI, the PCR product was cloned into *Eco*RI-digested YEp352 (YEp352C2C). Next, the 1.1-kb *cit1* fragment containing the promoter region and the first 85 codons of the Cit1p coding sequence was amplified by PCR from pLCS1 using primers P1 (5′ATGACCATGATTACGAATTC3′) and P3 (5′AACAAGGCCTTGAATTCCTCTCATACCACC3′) (Fig. 1) and digested with *Eco*RI. The *cit1* fragment was then ligated in the correct orientation into YEp352C2C partially digested with *Eco*RI upstream of

TABLE I. ***S. cerevisiae* strains and plasmids used in this study.**

Strain and plasmid	Relevant genotype	Reference or source
PSY37	*eu2-3 leu2-112 ura3-52 lys2-801*	(*22*)
PSY38	*cit1::LEU2 leu2-3 leu2-112 ura3-52 lys2-801*	(*21*)
PSY40	*cit2::URA3 leu2-3 leu2-112 ura3-52 lys2-801*	(*21*)
PSY44	*cit1::LEU2 cit2: :URA3 leu2-3 leu2-112 ura3-52 lys2-801*	(*21*)
MPY001	*cit1::LEU2 cit2: :ura3-508 leu2-3 leu2-112 ura3-52 lys2-801*	This study
W303a	*ura3-52 his3-200 ade2-101 trp1-901 leu2-3 leu2-112*	(*36*)
W303a-1	*pex5::URA3 ura3-52 his3-200 ade2-101 trp1-901 leu2-3 leu2-112*	P. B. Lazarow
W303a-2	*pex7::HIS3 ura3-52 his3-200 ade2-101 trp1-901 leu2-3 leu2-112*	P. B. Lazarow
pLCS1	*CIT1 LEU2*	(*21*)
pUCS2	*CIT2 URA3*	(*21*)
YEpCit1::Cit2	*cit1-85::cit2-392 URA3*	This study
YEpCit2::Cit1	*cit2-68::cit1-395 URA3*	This study
YEpCit1$_{(p)}$::GFP2	*cit1-p::gfp2 URA3*	This study
YEpCit1$_{(1-38)}$::GFP2	*cit1-38::gfp2 URA3*	This study
YEpCit1$_{(p)}$::GFP2-SKL	*cit1-p::gfp2-SKL URA3*	This study
YEpCit1$_{(1-38)}$::GFP2-SKL	*cit1-38::gfp2-SKL URA3*	This study
YEpCit2$_{(p)}$::GFP2	*cit2-p::gfp2 LEU2*	This study
YEpCit2$_{(p)}$::GFP2-SKL	*cit2-p::gfp2-SKL LEU2*	This study
YEpCit2$_{(1-8)}$::GFP2	*cit2-8::gfp2 LEU2*	This study
YEpCit2$_{(1-20)}$::GFP2	*cit2-20::gfp2 LEU2*	This study
YEpCit2$_{(1-65)}$::GFP2	*cit2-65::gfp2 LEU2*	This study
YEpCit2$_{(1-65)}$::GFP2-SKL	*cit2-65::gfp2-SKL LEU2*	This study
YCpCit2$_{(p)}$::GFP2	*cit2-p::gfp2 LEU2 CEN4*	This study
YCpCit2$_{(1-8)}$::GFP2	*cit2-8::gfp2 LEU2 CEN4*	This study
YCpCit2$_{(1-20)}$::GFP2	*cit2-20::gfp2 LEU2 CEN4*	This study
YCpCit2$_{(1-65)}$::GFP2	*cit2-65::gfp2 LEU2 CEN4*	This study

Downloaded from http://jb.oxfordjournals.org/ at Peking University on October 1, 2012

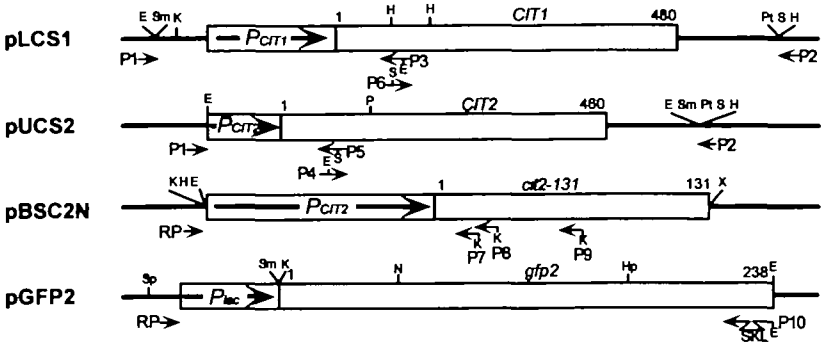

Fig. 1. **Design of the PCR primers used to amplify the DNA fragments encoding the N- and C-terminal segments of citrate synthases Cit1p and Cit2p, and for the construction of the cDNA encoding GFP2-SKL.** To facilitate in-frame fusions, *Eco*RI sites were installed in P3 and P4 primers, and *Sph*I sites in P5 and P6 primers by substitution of certain appropriate nucleotides that caused no change in the original amino acids sequences. In P7, P8, and P9 primers, *Kpn*I sites were installed; thus the PCR products amplified with these primers contained two additional codons for Val-Pro. Restriction enzyme sites: E, *Eco*RI; H, *Hin*dIII; Hp, *Hpa*I; K, *Kpn*I; N, *Nco*I; P, *Pvu*II; Pt, *Pst*I; S, *Sph*I; Sm, *Sma*I; Sp, *Sap*I; X, *Xba*I.

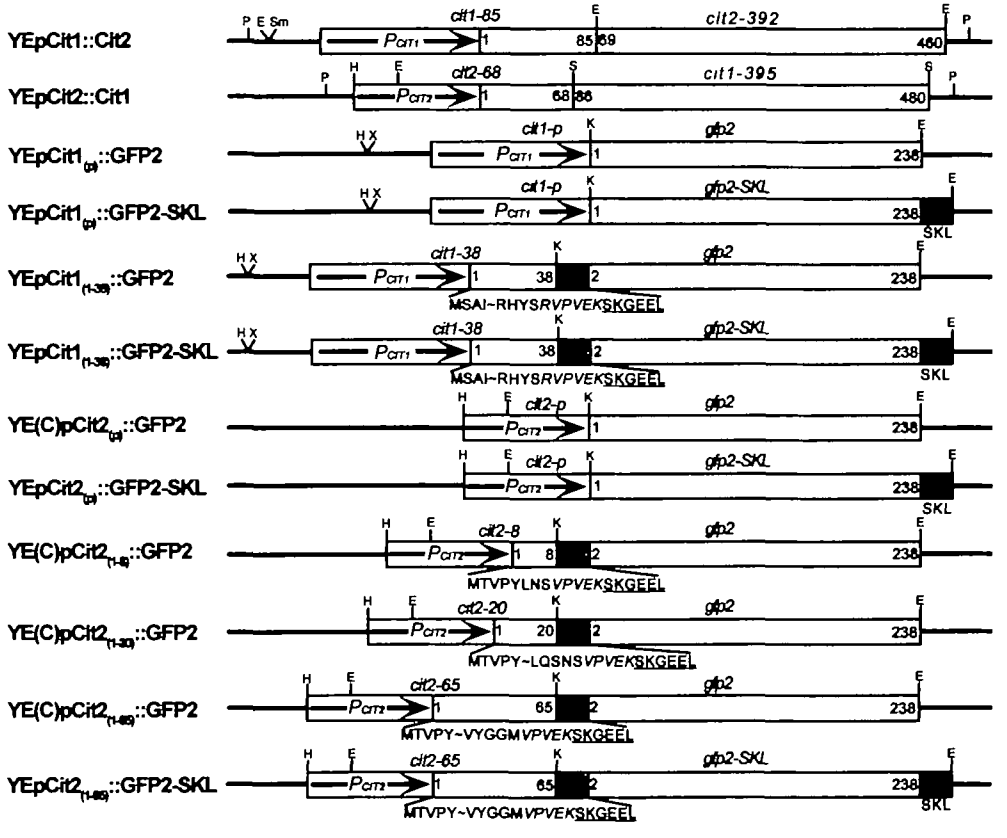

Fig. 2. **Structures of the chimeric genes encoding the N-terminal domain–swapped citrate synthases and the GFP fusions containing the N-terminal segments of citrate synthases.** The promoter regions of *CIT1* (P_{CIT1}) and *CIT2* (P_{CIT2}, including UAS_r sequence) are both designated by solid arrows. Numerals in each bar refer to the amino acid positions at the boundaries of the polypeptide segment encoded by the allele. Letters below each bar represent the amino acids at the indicated fusion protein junctions, and the underlined litters designate the N-terminal amino acid sequence of GFP. Restriction enzyme sites: E, *Eco*RI; H, *Hin*dIII; K, *Kpn*I; P, *Pvu*II; S, *Sph*I; Sm, *Sma*I; X, *Xba*I.

the 1.6-kb *cit2* fragment to yield YEpCit1::Cit2 (Fig. 2).

The hybrid gene for Cit2::Cit1 containing the 68–amino acid N-terminal segment of Cit2p fused to the 395–amino acid C-terminal segment of Cit1p, was constructed as follows. First, the 0.5-kb *cit2* fragment containing the promoter region and the N-terminal 68 codons of the Cit2p coding sequence was amplified from pUCS2 using primers P1 and P5 (5′TGGAATACCTCGCATGCCACCATATACCTG3′) (Fig. 1). After digestion with *Eco*RI and *Sph*I, the *cit2* fragment was cloned into *Eco*RI–*Sph*I–digested YEp352 (YEp352C2N). Next, the 1.6-kb *cit1* fragment containing the coding region for the C-terminal 392 amino acids of Cit1p was amplified from pLCS1 using primers P6 (5′AGCTTATGGTGGCATGCGAGGTATTAAAGG3′) and P2 (Fig. 1). The *cit1* fragment was then inserted in the correct orientation into *Sph*I-digested YEp352C2N downstream of the *cit2* fragment (YEp352C21).

To maximize the expression of Cit2::Cit1, the upstream activation site (UAS_r) of *CIT2* (*27*) was synthesized and inserted it into the upstream part of the hybrid gene. The mutually primed synthesis of UAS_r using *Taq* DNA polymerase was carried out in a reaction mixture containing a pair of primers [PU1 (5′TAAGCTTGCGGTGGTCATCGACTAGGGGCGAAGAGGTCACGACCTATTTTTTCTTGCAG3′) and PU2(5′CGAATTCTACGGAAAAGGTCACACTTTTTTTCTGCAAGAAA3′)] that share a 10-nt complementary region but lacking an additive template DNA. After *Hin*dIII–*Eco*RI digestion, the UAS_r fragment was cloned into *Hin*dIII–*Eco*RI–digested YEplac181 (*28*) to yield YEplacUAS. The 2.1-kb fragment containing *cit2::cit1* was

Downloaded from http://jb.oxfordjournals.org/ at Peking University on October 1, 2012

excised from YEp352C21 by digestion with *Eco*RI and *Pvu*II (partial). The resulting fragment was inserted into *Eco*RI–*Pvu*II (partial)–digested YEplacUAS downstream of UAS_r (YEplacUASC21). The 2.4-kb *Pvu*II *cit2-68::cit1-395* fragment (including UAS_r) was then excised from YEplacUASC21 and cloned into *Pvu*II-digested YEp352 to yield YEpCit2: :Cit1 (Fig. 2).

Construction of pGFP2 was accomplished by exchanging the 0.4-kb *Nco*I–*Hpa*I *gfp* fragment from pGFP (Clontech, Palo Alto, California, USA) with the corresponding region of *gfp2* (harboring Ser 65→Thr mutation) excised from pNEXδ-S65T (*29*). YEp352GFP2 was constructed by cloning the 0.75-kb *Sma*I–*Eco*RI *gfp2* fragment from pGFP2 into *Sma*I–*Eco*RI–digested YEp352. YEplacGFP2 was constructed by cloning the 1.0-kb *Sap*I–*Eco*RI *gfp2* fragment from pGFP2 into *Sap*I–*Eco*RI–digested YEplac181. YCplac-GFP2 was constructed by cloning the 0.75-kb *Kpn*I–*Eco*RI *gfp2* fragment from pGFP2 into *Kpn*I–*Eco*RI–digested YCplac111.

To construct the genes for Cit1::GFP2 fusion proteins, the 1.1-kb *Sma*I–*Hin*dIII *cit1* fragment from pLCS1 was cloned into pBluescript II KS(+) (Stratagene, La Jolla, California, USA) to yield pBSC1N. After digestion of pBSC1N with *Hin*dIII, serial deletion was carried out by treatment with exonuclease III (Takara Shuzo, Shiga) followed by digestion with S1 nuclease (Takara Shuzo). The shortened DNA was cleaved with *Xba*I, and the DNA fragments 0.8–1.1 kb in length were ligated into *Xba*I–*Sma*I–digested YEp352GFP2. The following two fusion constructs were selected: (i) $YEpCit1_{(p)}$::GFP2, a fusion of the 0.97-kb *cit1* fragment (including the promoter region from −10 to approx. −550) and *gfp2*; and (ii) $YEpCit1_{(1\text{-}38)}$::GFP2, a fusion of the 1.09-kb *cit1* fragment (including the promoter region and the coding sequence for the N-terminal 38 amino acids of Cit1p) and *gfp2*. To construct the fusion of the *CIT2* promoter region and *gfp2*, the 0.65-kb *Eco*RI-*Pvu*II *cit2* fragment from pUCS2 was ligated into *Eco*RI-*Sma*I–digested pBluescript II KS(+) (pBSC2N). After pBSC2N was cut with *Xba*I, serial deletion was carried out as described above. The shortened DNA was cut with *Hin*dIII, and the DNA fragments 0.2–0.3 kb in length were separated and cloned into *Hin*dIII-*Sma*I–digested YEplacGFP2. From the resulting hybrid genes, we selected a *cit2::gfp2* hybrid containing 0.25 kb of the *CIT2* promoter region from −12 to −260 (YEplacC20-GFP2). The hybrid gene was then excised with *Eco*RI, and cloned into *Eco*RI-digested YEplac-UAS downstream of UAS_r in the correct orientation to yield $YEpCit2_{(p)}$::GFP2 (Fig. 2).

Three chimeric genes that encode hybrid proteins of Cit2p and GFP2 containing varying numbers of N-terminal amino acids were constructed as follows. First, the 0.28-, 0.32-, and 0.45-kb *cit2* fragments were amplified individually from pBSC2N with primer RP (reverse primer, 5′AACAGCTATGACCATG3′) and either primer P7 (5′GGTACCGAATTTAGATAAGGAAC3′), P8 (5′GGTACCTGAATTTGATTGTAAATA3′), or P9 (5′GGTACCATACCACCATATACCTGTTCT3′), respectively (Fig. 1). The *cit2* fragments were cloned into the *Eco*RV site of pT7Blue(R) (Novagen, Madison, Wisconsin, USA), and then excised by *Hin*dIII–*Kpn*I double digestion and inserted into *Hin*dIII-*Kpn*I–digested YEplacGFP2 upstream of *gfp2* (YEplacC28-GFP2, YEplacC220-GFP2, and YEplacC265-GFP2). The three *cit2*: *gfp2* hybrid genes were then excised by digestion with *Eco*RI, and cloned individually into *Eco*RI-digested YEplacUAS downstream of UAS_r in the correct orientation to yield $YEpCit2_{(1\text{-}8)}$::GFP2, $YEpCit2_{(1\text{-}20)}$::GFP2, and $YEpCit2_{(1\text{-}65)}$::GFP2 (Fig. 2).

Each of the four *cit2::gfp2* hybrid genes was also assembled in a low-copy vector, YCplac111. To accomplish this, the 0.33-kb *cit2-p*, 0.36-kb *cit2-8*, 0.40-kb *cit2-20*, and 0.53-kb *cit2-65* fragments were excised by *Hin*dIII–*Kpn*I double digestion of $YEpCit2_{(p)}$::GFP2, $YEpCit2_{(1\text{-}8)}$::GFP2, $YEpCit2_{(1\text{-}20)}$::GFP2, and $YEpCit2_{(1\text{-}65)}$::GFP2, respectively, and cloned individually into *Hin*dIII–*Kpn*I–digested YCplac-GFP2 vector upstream of *gfp2* to yield $YCpCit2_{(p)}$::GFP2, $YCpCit2_{(1\text{-}8)}$::GFP2, $YCpCit2_{(1\text{-}20)}$::GFP2, and $YCpCit2_{(1\text{-}65)}$:: GFP2.

The gene for GFP2-SKL carrying a C-terminal PTS1 was amplified from pGFP2 by PCR using primers RP and P10 (5′CGAATTCTATAATTTTGATTTGTATAGTTCATC3′) (Fig. 1), and cloned into pT7Blue(R) (pT7GFP2-SKL).

To facilitate the exchange of *gfp2* with the 0.75-kb *Kpn*I–*Eco*RI *gfp2-SKL* fragment, additional *Kpn*I sites of $YEpCit1_{(p)}$::GFP2 and $YEpCit1_{(1\text{-}38)}$::GFP2 located upstream of the *CIT1* promoter region were eliminated by *Kpn*I digestion, treatment with T4 DNA polymerase, and self-ligation ($YEpCit1_{(p)}$::GFP2-K and $YEpCit1_{(1\text{-}38)}$::GFP2-K). The 0.75-kb *Kpn*I–*Eco*RI *gfp2-SKL* fragment from pT7GFP2-SKL was cloned into $YEpCit1_{(p)}$::GFP2-K and $YEpCit1_{(1\text{-}38)}$:: GFP2-K from which *gfp2* had been deleted by *Kpn*I–*Eco*RI digestion to yield $YEpCit1_{(p)}$::GFP2-SKL and $YEpCit1_{(1\text{-}38)}$:: GFP2-SKL (Fig. 2).

To construct $YEpCit2_{(p)}$::GFP2-SKL and $YEpCit2_{(1\text{-}65)}$:: GFP2-SKL (Fig. 2), the *Kpn*I–*Eco*RI *gfp2-SKL* fragment from pT7GFP2-SKL was inserted into *Kpn*I–*Eco*RI(partial)–digested $YEpCit2_{(p)}$::GFP2 and $YEpCit2_{(1\text{-}65)}$::GFP2, respectively, from which *gfp2* had been eliminated.

To construct the expression cassettes of *S. cerevisiae* Cta1p (catalase A) and Cit1p used to immunize rabbits to raise anti-Cta1p and anti-Cit1p antibodies, respectively, partial *CTA1* (*30*) and whole *CIT1* ORFs were amplified by PCR. Amplification of the *S. cerevisiae* CTA1 fragment was carried out using a pair of primers, P11 (5′CCCAACGTATTGGGGAACTAGGC3′) and P12 (5′GGGATGTTGCCCAATGATAAGGG3′). The PCR product was cloned into pT7Blue(R) to yield pT7Cta1, from which the 1.2-kb *Nco*I–*Xho*I *CTA1* fragment was excised and cloned into the *Nco*I–*Xho*I–digested pET21b (Novagen) to give pETCta1. The *CIT1* ORF was also amplified using a pair of primers, P13 (5′GGATCCGATGTCAGCGATATTATCA3′) and P14 (5′CTCGAGGTTCTTACTTTCGATTTT3′), and the 1.4-kb PCR product was cloned into pT7Blue(R) to give pT7Cit1. Then the *Bam*HI–*Xho*I *CIT1* fragment was excised and cloned into the *Bam*HI–*Xho*I–digested pET21b to yield pETCit1.

Confocal Microscopy—For confocal microscopic observations, yeast cells were stained with 100 nM MitoTracker Red CMXRos (Molecular Probes, Eugene, Oregon, USA) for 30 min at 37°C and fixed with 3% formaldehyde for 30 min. Cells and organelles of *S. cerevisiae* strains were examined under a Leica TCS NT confocal system (Leica, Heerbrugg, Switzerland) using an FITC filter set (450–490 excitation filter) or a TRICT filter set (540–560 excitation filter).

Cell Fractionation—For cell fractionation, one gram (wet weight) of washed yeast cells were suspended in 7 ml of 0.1 M Tris-SO_4 buffer (pH 8.5) containing 10 mM dithiothreitol and incubated at 30°C for 30 min. After a rinse with 1.2 M

Downloaded from http://jb.oxfordjournals.org/ at Peking University on October 1, 2012

sorbitol, the cells were resuspended in isotonic buffer (1.2 M sorbitol in 20 mM potassium phosphate, pH 7.4) and treated with lyticase (1,000 to 2,500 units/g cell wet weight; Sigma, St. Louis, Missouri, USA) at 30°C for 1.5 h. The resulting spheroplasts were harvested by centrifugation (3,000 ×*g*), resuspended in lysis buffer (0.6 M sorbitol, 1 mM KCl and 0.5 mM EDTA in 5 mM MES-KOH buffer, pH 6.0), and homogenized in a Dounce glass homogenizer. The cell debris was removed by centrifugation (1,500 ×*g*, 10 min), and the organelles were harvested (25,000 ×*g*, 20 min). The organelles were resuspended in 5 mM MES-KOH buffer (pH 6.0) containing 0.24 M sucrose and 1 mM EDTA and fractionated by ultracentrifugation through a step gradient prepared with 17, 25 and 35% Nycodenz solutions in the same buffer. Ultracentrifugation (Beckman LE-80) was carried out in a SW55Ti rotor at 112,000 ×*g* for 90 min at 4°C. Each fraction from the gradient was diluted 5-fold with 5 mM MES-KOH buffer (pH 6.0) containing 0.24 M sucrose and 1 mM EDTA, and the Nycodenz was removed by centrifugation at 25,000 ×*g* for 20 min. For immunoblotting and enzyme assay, the organelles were ruptured by adding Triton X-100 to a concentration of 1%.

Enzyme Assay—Citrate synthase was assayed by the 5,5′-dithiobis-(2-nitrobenzoic acid) (DTNB) method (*31*). Cytochrome *c* oxidase (*32*) and catalase (*33*) activities were measured spectrophotometrically.

Spectrofluorometric Analysis—The intensity of green fluorescence was estimated with a spectrofluorometer (FP770, Jasco, Tokyo) under the following conditions: excitation wavelength, 490 nm; emission wavelength, 510 nm.

Immunoblotting—Immunoblotting was carried out by the enhanced chemiluminescence method (ECL; Amersham). Primary antibodies were the mouse monoclonal anti-Cox3p (cytochrome *c* oxidase subunit III of *S. cerevisiae*; Molecular probes), rabbit anti-GFP (Clontech), rabbit anti-Cta1p, and rabbit anti-Cit1p antibody. Rabbit anti-Cta1p and anti-Cit1p antisera were prepared from rabbits immunized, respectively, with Cta1p and Cit1p overexpressed in *E. coli* and fractionated by SDS-PAGE. Secondary antibodies were horseradish peroxidase–conjugated anti-rabbit IgG and anti-mouse IgG (Kirkegaard and Perry, Gaithersburg, Maryland, USA).

RESULTS

Physiological Activity of the N-Terminal Domain–Swapped Citrate Synthases—To assess the physiological activity of the two N-terminal domain–swapped citrate synthases, we transformed the *cit1 cit2* double disruptant (MPY001) individually with YEpCit1::Cit2 and YEpCit2::Cit1 (Fig. 2). As expected, the *cit1* cit2 double disruptant grew on YNB/UGL (YNB with uridine, glutamate, and leucine); however, it failed to grow on YNB, YNB/UL (YNB with uridine and leucine), YNB/GL (YNB with glutamate and leucine), or YEP/A (YEP with acetate) plates (Fig. 3). These observations confirm that the double disruptant has auxotrophy both for uracil and glutamate, as well as an inability to utilize acetate as a sole carbon source. The glutamate auxotrophy reflects double disruption of the two citrate synthase genes (*cit1::LEU2* and *cit2::ura3-508*) (*17*). In contrast to the *cit1 cit2* double mutant, both YEpCit1::Cit2 and YEpCit2::Cit1 transformants grew very well on YNB medium (Fig. 3), which indicates that the glutamate auxotrophy can be complemented by either of the two hybrid genes, *cit1::cit2* or *cit2::cit1*. This result indicates that both of the N-terminal domain–swapped citrate synthases, when expressed in the double disruption strain, can fulfill the role of supplying adequate amounts of citrate which is converted into α-ketoglutarate, the precursor for glutamate biosynthesis, *via* the TCA cycle. On YEP/A medium, YEpCit1::Cit2 transformants exhibited nearly the same growth rate as the wild-type strain (*CIT1 CIT2*), while YEpCit2::Cit1 transformants showed no growth (Fig. 3). This result shows that the *cit1::cit2* hybrid gene can support growth on acetate, while the *cit2::cit1* hybrid gene can not. It is thus suggested that on YEP/A medium, the CIT1-promoter in the *cit1::cit2* hybrid gene supports the synthesis of an adequate amount of Cit1::Cit2 protein required for growth on low-energy nonfermentable carbon sources such as acetate, while the CIT2 promoter in *cit1::cit2* does not (*19, 34*)

An Atypical Signal for Both Mitochondrial and Peroxisomal Targeting in the N-Terminal Region of Cit2p—To analyze the intracellular localization of the two N-terminal

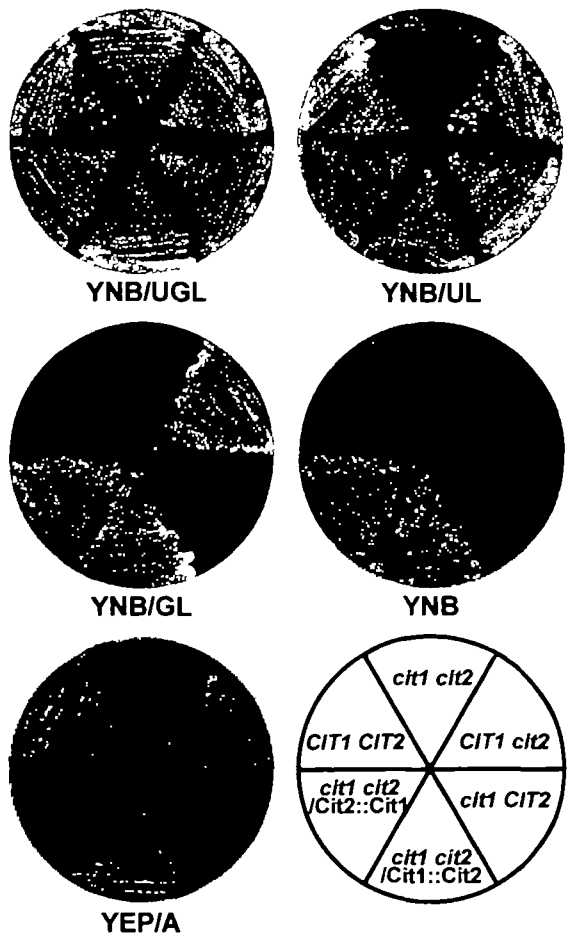

Fig. 3. **Functional complementation of the *cit1 cit2* double mutation by the N-terminal domain–swapped citrate synthases.** The cells of PSY37 (*CIT1 CIT2*), MPY001 (*cit1 cit2*), PSY40 (*CIT1 cit2*), PSY38 (*cit1 CIT2*), MPY001/YEpCit1::Cit2, and MPY001/YEpCit2::Cit1, were grown on YNB, YNB/UGL (YNB with uridine, glutamate and leucine), YNB/UL (YNB with uridine and leucine), YNB/GL (YNB with glutamate and leucine), or YEP/A (YEP with acetate).

Downloaded from http://jb.oxfordjournals.org/ at Peking University on October 1, 2012

domain–swapped citrate synthases, we carried out cell fractionation of the *cit1 cit2* double mutant and its transformed strains. The resulting subcellular fractions were then analyzed for catalase and cytochrome c oxidase activities. In each case, while the peak of cytochrome c oxidase activity was localized in fraction #4 (bottom part of the 17% Nycodenz layer), the peak catalase activity was detected in fraction #10 (bottom part of the 25% layer) (Fig. 4). These observations confirm that mitochondria and peroxisomes were concentrated in fractions #4 and #10, respectively. The distribution of the wild type and two N-terminal domain–swapped citrate synthases was analyzed by measuring the enzyme activity in each fraction. In the cell lysate from the wild-type strain (*CIT1 CIT2*), the highest amount of citrate synthase activity was detected in the mitochondrial fraction, and a small amount of the activity was localized in the peroxisomal fraction. Lysates of the *cit1* and *cit2* mutants had peak citrate synthase activities in the peroxisomal and mitochondrial fractions, respectively. As expected, no citrate synthase peak was identified in cell lysates of the *cit1 cit2* double mutant. These results indicate that the isofunctional citrate synthases are targeted separately to two distinct intracellular organelles: Cit1p to mitochondria and Cit2p to peroxisomes. In the cell lysates of YEpCit1::Cit2 and YEpCit2::Cit1 transformants, citrate synthase activity was detected in both the mitochondrial and peroxisomal fractions. This result suggests that each of the two hybrid proteins, Cit1::Cit2 and Cit2::Cit1, is transported into both mitochondria and peroxisomes. It also indicates that the hybrid proteins do have citrate synthase activity, although the levels are quite low compared with those of the wild type enzymes.

We also used immunoblotting to analyze the proteins in the mitochondrial and peroxisomal fractions of various yeast strains (Fig. 5). The wild type strain showed a single positive band of ~50 kDa in both the mitochondrial and peroxisomal fractions. In contrast, the *cit1* disruptant showed a single protein band with a similar molecular mass only in the peroxisomal fraction, while the *cit2* disruptant showed a single ~50 kDa protein band in the mitochondrial fraction alone. These results indicate that the anti-Cit1p antibody recognizes Cit2p as well as Cit1p. Such

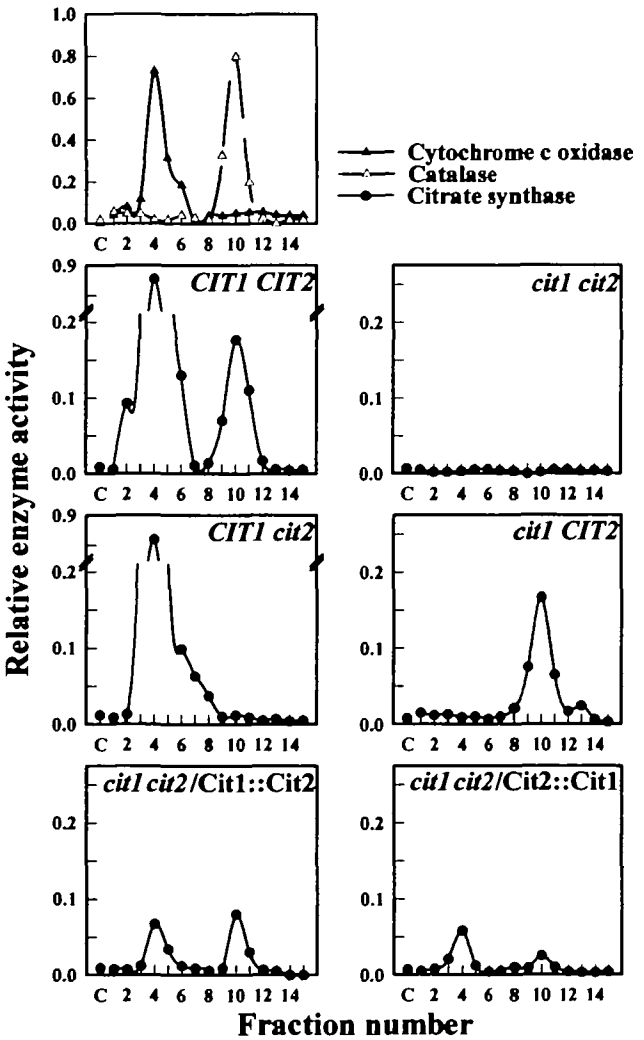

Fig. 4. **Analysis of subcellular distribution of the N-terminal domain–swapped citrate synthases by cell fractionation.** Homogenized lysates from PSY37 (*CIT1 CIT2*), MPY001 (*cit1 cit2*), PSY40 (*CIT1 cit2*), PSY38 (*cit1 CIT2*), MPY001/YEpCit1::Cit2, and MPY001/YEpCit2::Cit1 cells were fractionated by ultracentrifugation. In addition to the cytosolic fraction (C), a total of 15 equal fractions of the Nycodenz gradient were siphoned from the top of the centrifuge tube. After the organelles were ruptured, the citrate synthase activity in each fraction was measured. The locations of mitochondria and peroxisomes from the *S. cerevisiae* PSY37 strain were monitored by the activities of cytochrome *c* oxidase and catalase, respectively.

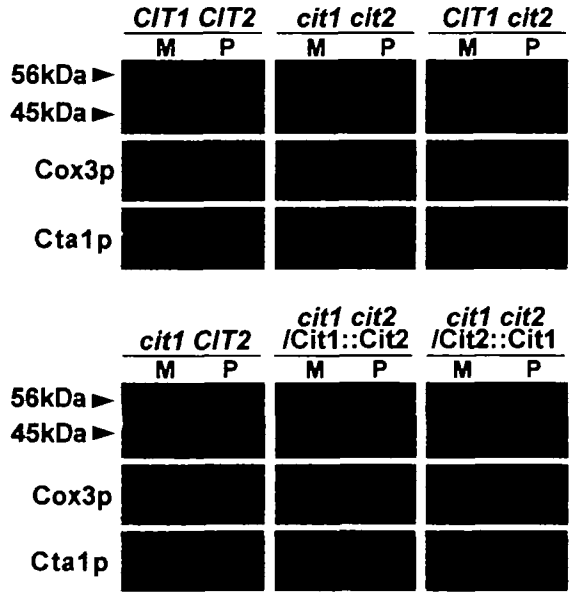

Fig. 5. **Immunoblot analysis of the subcellular distribution of the N-terminal domain–swapped citrate synthases.** Mitochondria (M) and peroxisomes (P) from PSY37 (*CIT1 CIT2*), MPY001 (*cit1 cit2*), PSY40 (*CIT1 cit2*), PSY38 (*cit1 CIT2*), MPY001/YEpCit1::Cit2, and MPY001/YEpCit2::Cit1 cells were fractionated by ultracentrifugation. Proteins contained in each 3-μl aliquot of mitochondrial (out of approx. 30 μl) and peroxisomal (out of approx. 30 μl) fractions prepared from one gram of cells were separated by SDS-PAGE in a 10% acrylamide gel. The *S. cerevisiae* citrate synthases and their derivatives were detected with the use of rabbit anti-Cit1p as a primary antibody, cytochrome *c* oxidase with mouse monoclonal anti-Cox3p, and catalase A with rabbit anti-Cta1p.

Downloaded from http://jb.oxfordjournals.org/ at Peking University on October 1, 2012

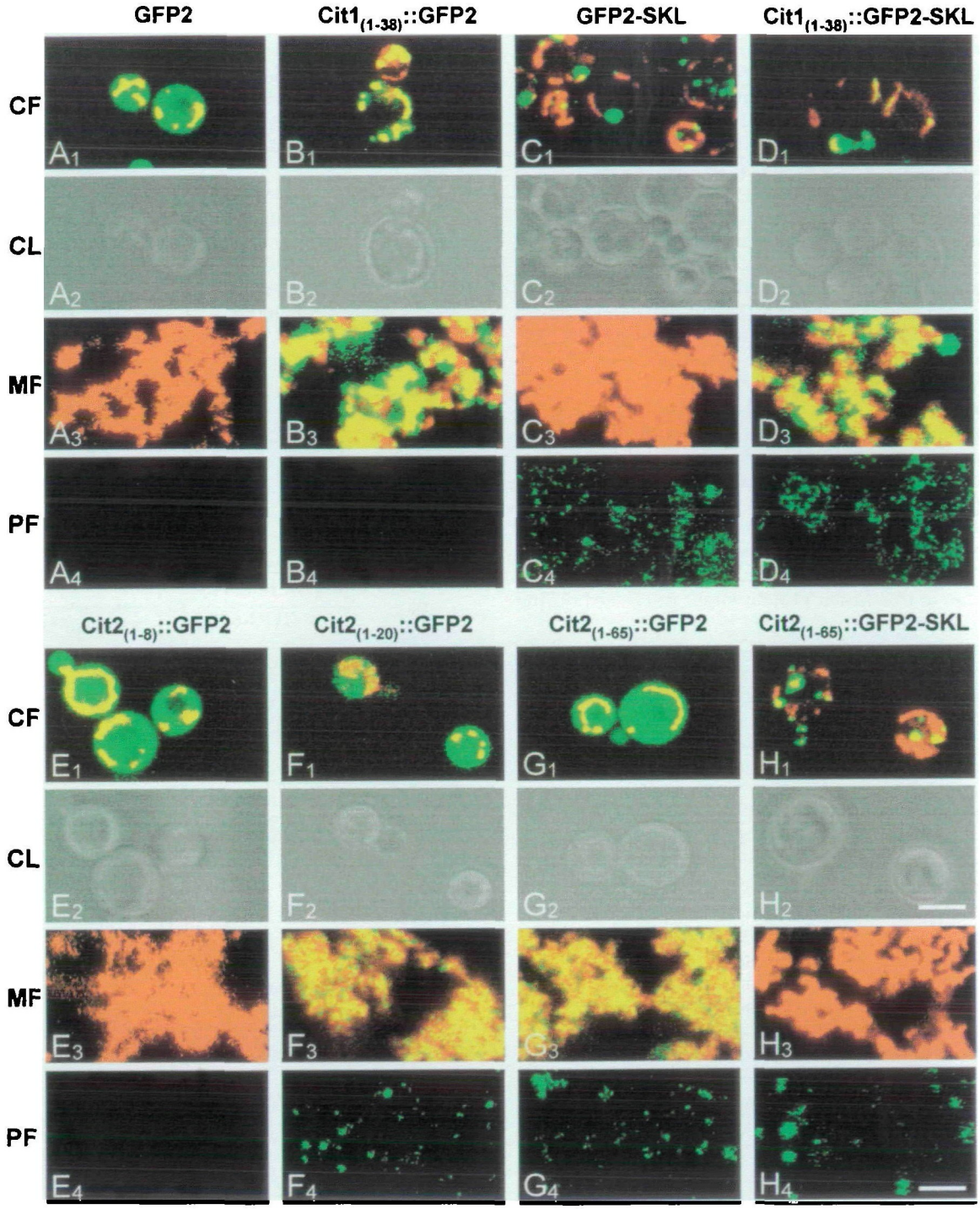

Fig. 6. **Confocal microscopic observation of the subcellular distribution of the GFP2 fusion proteins.** Cells of PSY37 (*CIT1 CIT2*) containing YEpCit2$_{(p)}$::GFP2 (A_{1-4}), YEpCit1$_{(1-38)}$::GFP2 (B_{1-4}), YEpCit2$_{(p)}$::GFP2-SKL (C_{1-4}), YEpCit1$_{(1-38)}$::GFP2-SKL (D_{1-4}), YEpCit2$_{(1-8)}$::GFP2 (E_{1-4}), YEpCit2$_{(1-20)}$::GFP2 (F_{1-4}), YEpCit2$_{(1-65)}$::GFP2 (G_{1-4}), or YEpCit2$_{(1-65)}$::GFP2-SKL (H_{1-4}) were stained with Mito Tracker Red CMXRos, fixed with formaldehyde, and observed using FITC and TRITC filters. Mitochondria and peroxisomes fractionated by ultracentrifugation were observed similarly. Fluorescent images of cells (CF), mitochondria (MF), and peroxisomes (PF) are presented together with a light image of the cells (CL). All the fluorescent images were generated by overlapping the GFP images (by FITC filter) with the MitoTracker Red CMXRos images (by TRITC filter). Yellow areas indicate the overlap of the green fluorescence of GFP and the red fluorescence of MitoTracker Red CMXRos. Scale bars, 5 μm (CF, CL); 3 μm (MF, PF).

results were expected because of the high degree of homology (81%) between the amino acid sequences of Cit1p and Cit2p (*19*).

As expected, no visible protein band recognized by the anti-Cit1p antibody was observed in any of the organelle fractions from the lysate of the *cit1 cit2* double disruptant. On the contrary, two forms of the Cit1::Cit2 derivatives with different molecular masses (~53 and ~50 kDa) were

Downloaded from http://jb.oxfordjournals.org/ at Peking University on October 1, 2012

detected in both the mitochondrial and peroxisomal fractions of the YEpCit1::Cit2 transformant. In the mitochondrial fraction, the smaller protein (~50 kDa) seems to be formed by proteolytic cleavage of the N-terminal MTS during the import process. This result is consistent with our previous finding that the 37 N-terminal amino acids of Cit1p are removed by cleavage [R(35)-H-Y↓(38)] in the process of mitochondrial targeting (*21*, *22*). The minor band is presumed to be due to the presence of the full-length form (~53 kDa), which is on its way to the mitochondrial matrix but yet to be cleaved. In the peroxisomal fraction, a majority of the fusion protein was detected as the full-length form, which supports the notion that the peroxisomal targeting process is guided by the C-terminal PTS1 without any proteolytic cleavage. The minor smaller species is presumed to be formed by proteolytic cleavage of the N-terminal segment that takes place either before or after the fusion protein enters the peroxisomal targeting process.

The molecular masses of the mature forms of Cit2::Cit1 detected in the mitochondrial and peroxisomal fractions of YEpCit2::Cit1 transformants were estimated to be ~50 kDa. Thus there is a difference of ~2-kDa between the measured molecular masses of the mature forms of Cit2::Cit1 and the predicted value derived from the ORF of the corresponding hybrid gene. This result suggests that the N-terminal region of this fusion protein might be cleaved during the targeting process.

It is not surprising that Cit1: :Cit2 is targeted into both mitochondria and peroxisomes, because this fusion protein contains both the N-terminal MTS of Cit1p and the C-terminal PTS1 (the SKL sequence) of Cit2p. The C-terminal SKL sequence of Cit2p has been shown to be necessary for the correct targeting of the enzyme into peroxisomes using a C-terminal deletion mutant (*34*). In contrast, it was not at all expected that Cit2::Cit1 would be transported into both organelles, as no typical organelle targeting signals exist in the N-terminal region of Cit2p or the C-terminal region of Cit1p. Thus it appears that an atypical, cryptic signal for both mitochondrial and peroxisomal targeting exists in the N-terminal part of Cit2p. This explanation is in partial agreement with the demonstration of Singh *et al.* (*34*) that Cit2p contains a cryptic MTS in its N-terminal region. However, there are no reports that suggest the potential function of the N-terminal region of Cit2p as a PTS.

Function of the N-Terminal Segment of Cit2p as a Cleavable Targeting Signal for Both Peroxisomal and Mitochondrial Protein Import—In order to obtain more definitive evidence that the N-terminal region of Cit2p can function as a signal for both mitochondrial and peroxisomal targeting, we constructed hybrid genes for fusion proteins containing varying lengths of the Cit2p or Cit1p N-terminal segment fused to the reporter protein GFP2 or GFP2-SKL. We then individually transformed the wild-type strain (PSY37) with high-copy plasmids containing the hybrid genes (Fig. 2), and the resulting transformants were subjected to subcellular localization of the fusion proteins by (i) confocal microscopic observation of intact cells and fractionated organelles (Fig. 6); (ii) spectrofluorometric analysis of the organelles (Fig. 7); and (iii) immunoblotting (Fig. 8).

Transformants harboring either YEpCit2$_{(p)}$::GFP2 or YEpCit1$_{(p)}$::GFP2 (data not shown) showed an obvious cytoplasmic distribution of GFP2 (Fig. 6A$_{1,2}$). No visible green fluorescence was observed in either mitochondria or peroxisomes fractionated by ultracentrifugation (Fig. 6A$_{3,4}$). In addition, spectrofluorometric analysis of the mitochondrial and peroxisomal fractions showed no detectable green fluorescence (Fig. 7), and a single positive protein band (27 kDa) was observed only in the cytoplasmic fraction by immunoblotting (Fig. 8). These results indicate that intact GFP2 is not imported into either mitochondria or peroxisomes.

In YEpCit1$_{(1\text{-}38)}$::GFP2 transformants, green fluorescence was localized to organelles that were stained with Mito Tracker Red CMXRos (Fig. 6B$_{1\text{-}4}$) and concentrated at the bottom part of the 17% Nycodenz layer after ultracentrifugation (Fig. 7). These results indicate that Cit1$_{(1\text{-}38)}$::GFP2 is targeted into mitochondria, and, thus, that the N-terminal

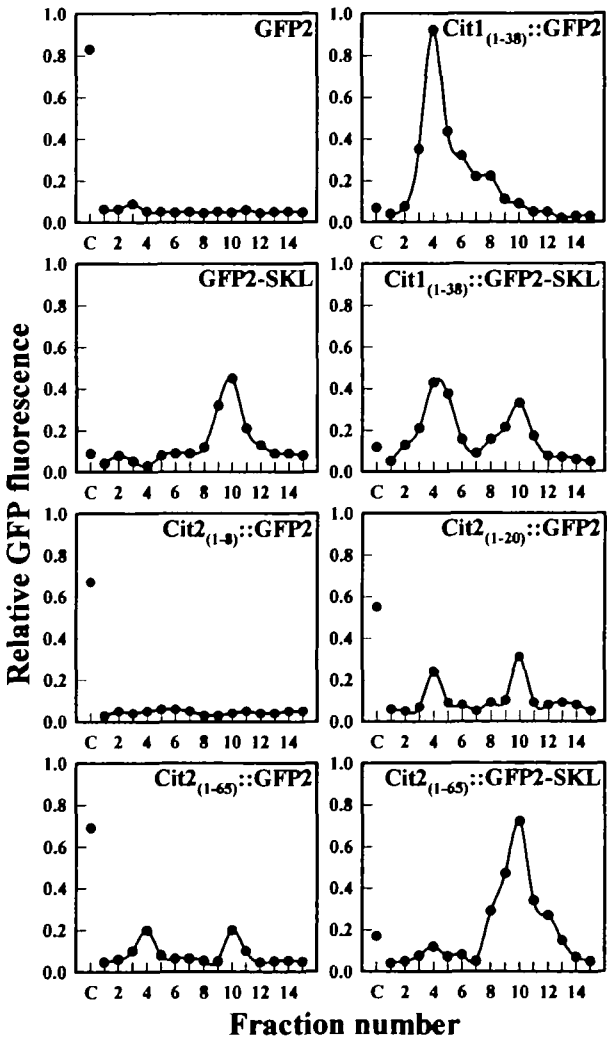

Fig. 7. **Analysis of the subcellular distribution of GFP2 fusion proteins by cell fractionation.** Homogenized cell lysates of PSY37 (*CIT1 CIT2*) containing YEpCit2$_{(p)}$::GFP2, YEpCit1$_{(1\text{-}38)}$::GFP2, YEpCit2$_{(p)}$::GFP2-SKL, YEpCit1$_{(1\text{-}38)}$::GFP2-SKL, YEpCit2$_{(1\text{-}8)}$::GFP2, YEpCit2$_{(1\text{-}20)}$::GFP2, YEpCit2$_{(1\text{-}65)}$::GFP2, or YEpCit2$_{(1\text{-}65)}$::GFP2-SKL were fractionated by ultracentrifugation. In addition to the cytosolic fraction (C), a total of 15 equal fractions of the Nycodenz gradient were siphoned from the top. After the organelles were ruptured, the fluorescence intensity was measured using a spectrofluorometer. Excitation wavelength, 488 nm; emission wavelength, 510 nm.

Downloaded from http://jb.oxfordjournals.org/ at Peking University on October 1, 2012

38 amino acids function as an MTS even when fused to a heterologous protein. On the other hand, GFP2-SKL expressed in either YEpCit2$_{(p)}$::GFP2-SKL or YEpCit1$_{(p)}$::GFP2-SKL (data not shown) transformants was effectively localized to spherical organelles that showed no red fluorescence (Fig. 6C$_{1-4}$) and were concentrated at the bottom part of the 25% Nycodenz layer (Fig. 7). These results confirm that GFP2-SKL is targeted into peroxisomes, and, thus, the C-terminal SKL sequence successfully functions as a PTS even when it is attached to a heterologous protein. As expected, YEpCit1$_{(1-38)}$::GFP2 and YEpCit2$_{(p)}$::GFP2-SKL transformants yielded appropriately sized protein bands in the mitochondrial and peroxisomal fractions, respectively (Fig. 8). The fusion protein detected in the mitochondrial fraction of YEpCit1$_{(1-38)}$::GFP2 transformants showed a molecular mass similar to that of GFP2 (27 kDa). This observation supports the notion that the N-terminal 37 amino acids of Cit1$_{(1-38)}$::GFP2 are cleaved in the process of

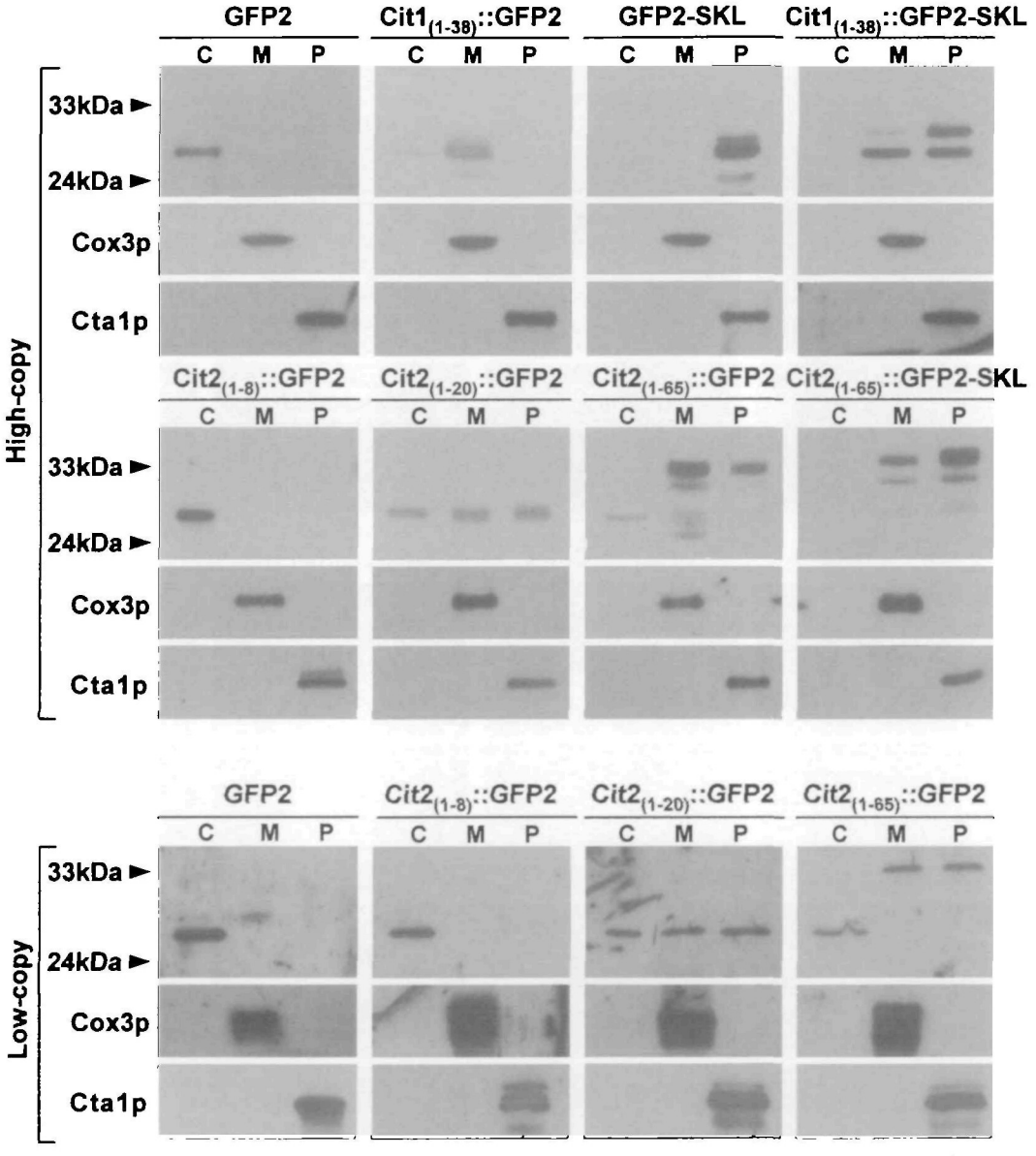

Fig. 8. **Immunoblot analysis of the subcellular distribution of the GFP2 fusion proteins.** Homogenized cell lysates of PSY37 (*CIT1 CIT2*) containing one of the high-copy (YEpCit2$_{(p)}$::GFP2, YEpCit1$_{(1-38)}$::GFP2, YEpCit2$_{(p)}$::GFP2-SKL, YEpCit1$_{(1-38)}$::GFP2-SKL, YEpCit2$_{(1-8)}$::GFP2, YEpCit2$_{(1-20)}$::GFP2, YEpCit2$_{(1-65)}$::GFP2, and YEpCit2$_{(1-65)}$: :GFP2-SKL) or low-copy plasmids (YCpCit2$_{(p)}$::GFP2, YCpCit2(1-8)::GFP2, YCpCit2(1-20)::GFP2, and YCpCit2(1-65):: GFP2) were fractionated by ultracentrifugation to yield cytosolic (C), mitochondrial (M), and peroxisomal (P) fractions. In the case of high-copy transformants, the proteins contained in each 3-μl aliquot of cytosolic (out of approx. 1,500 μl), mitochondrial (out of approx. 30 μl), and peroxisomal fractions (out of approx. 30 μl) prepared from 1 g of yeast cells were separated by SDS-PAGE in a 12.5% acrylamide gel. In the cases of low-copy transformants, amounts approx. 10-times larger than those of the high-copy transformants were loaded. However, in the mitochondrial (M) and peroxisomal lanes (P) for Cox3p and Cta1p detection, respectively, in which the amounts of corresponding marker enzymes exceeded the range for proper positive signal development, the amounts of samples were adjusted to approx. 9 μl. The GFP2 fusion proteins were detected using rabbit anti-GFP as a primary antibody, cytochrome *c* oxidase with mouse monoclonal anti-Cox3p, and catalase A with rabbit anti-Cta1p.

Downloaded from http://jb.oxfordjournals.org/ at Peking University on October 1, 2012

mitochondrial targeting, as in the case of the wild type Cit1p (*22*).

$Cit1_{(1-38)}$::GFP2-SKL was evenly localized to both mitochondria and peroxisomes (Figs. $6D_{1-4}$, 7, and 8). This indicates that, as with Cit1::Cit2 (Figs. 4 and 5), the MTS of Cit1p and PTS1 of Cit2p in $Cit1_{(1-38)}$::GFP2-SKL are equally

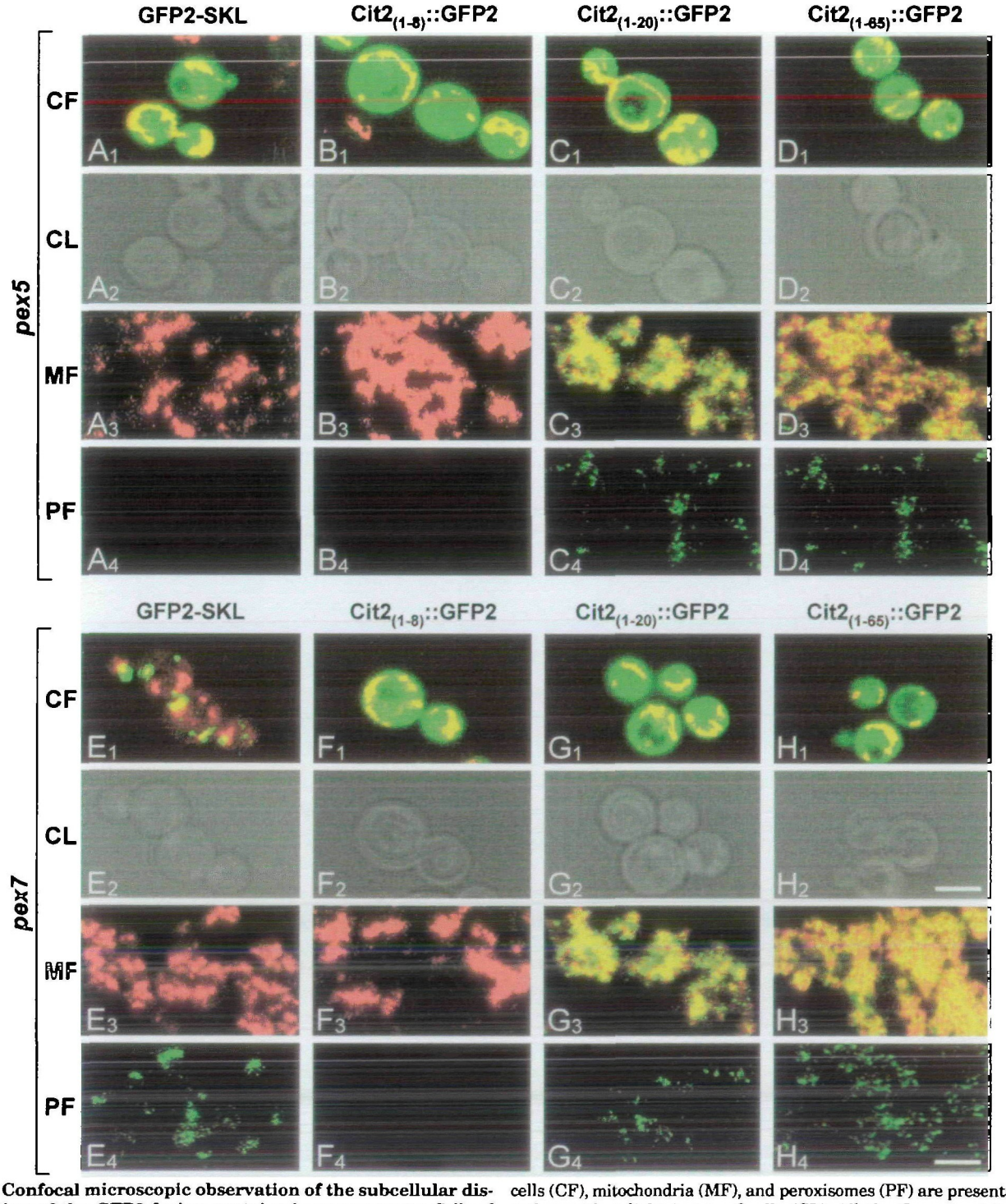

Fig. 9. Confocal microscopic observation of the subcellular distribution of the GFP2 fusion proteins in *pex* mutants. Cells of W303a-1 (*pex5*) and W303a-2 (*pex7*) containing $YEpCit2_{(1-8)}$::GFP2 (A_{1-4}, E_{1-4}), $YEpCit2_{(1-20)}$::GFP2 (B_{1-4}, F_{1-4}), $YEpCit2_{(1-65)}$::GFP2 (C_{1-4}, G_{1-4}), or $YEpCit2_{(p)}$::GFP2-SKL (D_{1-4}, H_{1-4}) were stained with Mito Tracker Red CMXRos, fixed with formaldehyde, and observed using FITC and TRITC filters. Mitochondria and peroxisomes fractionated by ultracentrifugation were observed similarly. Fluorescent images of cells (CF), mitochondria (MF), and peroxisomes (PF) are presented together with a light image of cells (CL). All the fluorescent images were generated by overlapping the GFP images (by the FITC filter) with the MitoTracker Red CMXRos images (by the TRITC filter). Yellow colored areas indicate the overlap of the green fluorescence of GFP and the red fluorescence of MitoTracker Red CMXRos. Scale bars, 5 μm (CF, CL); 3 μm (MF, PF).

Downloaded from http://jb.oxfordjournals.org/ at Peking University on October 1, 2012

functional as organelle targeting signals. The molecular mass of $Cit1_{(1-38)}$::GFP2-SKL in mitochondria is equivalent to the expected value (~27 kDa), suggesting that cleavage of the N-terminal MTS takes place during the import process. The ~31 kDa band detected in the mitochondrial fraction is presumed to be due to the presence of $Cit1_{(1-38)}$::GFP2-SKL molecules being targeted to mitochondria but yet to be cleaved. Two forms of GFP2 derivatives with different molecular masses (~27 and ~31 kDa) were identified in the peroxisomes of YEpCit1$_{(1-38)}$::GFP2-SKL transformants (Fig. 8). The larger species is thought to be the full-length form of the fusion protein, and the smaller one to be the processed form produced by the removal of the MTS, which takes place either before or after its entrance into peroxisomes guided by the PTS1.

Confocal micrographs of intact yeast cells and fractionated organelles from YEpCit2$_{(1-8)}$::GFP2 transformants, showed that $Cit2_{(1-8)}$::GFP2 is not targeted to either mitochondria or peroxisomes but evenly distributed throughout the cytoplasm (Figs. 6E_{1-4} and 7). On the contrary, both the purified mitochondria and peroxisomes from the transformants harboring either YEpCit2$_{(1-20)}$::GFP2 or YEpCit2$_{(1-65)}$::GFP2 showed green fluorescence (Figs. 6, $F_{3,4}$ and $G_{3,4}$, and 7), although their intact cells did not exhibit distinguishable green fluorescent organelles against the fluorescent cytoplasmic background (Fig. 6, $F_{1,2}$ and $G_{1,2}$). In addition, the green fluorescence of the organelles was not affected at all by treatment with proteinase K (25 mg/ml) for 30 min at 30°C (data not shown). These observations support $Cit2_{(1-20)}$::GFP2 and $Cit2_{(1-65)}$::GFP2 being targeted to both mitochondria and peroxisomes, as well as being spread throughout the cytoplasm. Thus the N-terminal region of Cit2p appears to function as an ambidextrous targeting signal for both mitochondria and peroxisomes, although it is relatively less efficient than the authentic targeting signals (that is, the C-terminal PTS1 and N-terminal MTS). Furthermore, it turns out that more than 8 N-terminal amino acids of Cit2p are required for the fusion proteins to be targeted to either organelle and that the first 20 amino acids are sufficient to constitute such a cryptic ambidextrous targeting signal.

The molecular masses of the mature forms of $Cit2_{(1-20)}$::GFP2 imported into mitochondria and peroxisomes were both estimated to be ~27 kDa (Fig. 8). This value is smaller by ~2 kDa than the molecular mass predicted from the ORF of the corresponding hybrid gene. Similarly, mature forms of $Cit2_{(1-65)}$::GFP2 imported into mitochondria and peroxisomes were both shown to be ~33 kDa (Fig. 8), which is also smaller by ~2 kDa than the molecular mass derived from the corresponding ORF. It is thus quite probable that 15 to 20 N-terminal amino acids of the two fusions are removed during their import into organelles. This is consistent with the previous suggestion that the 15 N-terminal amino acids of Cit2p might be cleaved during the peroxisomal targeting process (*22*).

In YEpCit2$_{(1-65)}$::GFP2-SKL transformants, only peroxisomes, but not mitochondria, showed green fluorescence in the confocal micrographs (Fig. 6H_{1-4}). However, immunoblotting analysis revealed a small amount of $Cit2_{(1-65)}$::GFP2-SKL targeted to mitochondria despite the presence of the C-terminal PTS1 (Fig. 8). These results thus support the notion that the N-terminal sequence of Cit2p retains its capability as an MTS, even though PTS1 plays a dominant role in the targeting process of the fusion protein to peroxisomes. In contrast, wild type Cit2p was shown to be targeted exclusively to peroxisomes by both the citrate synthase assay (Fig. 4) and immunoblotting (Fig. 5). Therefore, in the case of wild type Cit2p, the dominance of PTS1 over the N-terminal segment appears to be nearly absolute.

Unexpectedly, each of the YEpCit1$_{(1-38)}$::GFP2, YEpCit2$_{(1-20)}$::GFP2 and YEpCit2$_{(1-65)}$::GFP2 transformants showed a single protein band with a molecular mass of ~27 kDa in the cytoplasmic fraction (Fig. 8). This observation suggests that the fluorescent fusion proteins that remain in the cytoplasm do not retain their own full-length form, but rather exist as smaller derivatives. These truncated cytoplasmic proteins may be formed by posttranslational proteolytic cleavage of the N-terminal segments prior to entering the sorting process.

The intracellular localization of GFP2 and some of its fusion proteins was also analyzed by immunoblotting in transformants containing one of the low copy recombinant plasmids, YCpCit2$_{(p)}$::GFP2, YCpCit2$_{(1-8)}$::GFP2, YCpCit2$_{(1-20)}$::GFP2, or YCpCit2$_{(1-65)}$::GFP2. As shown in Fig. 8, $Cit2_{(1-20)}$::GFP2 and $Cit2_{(1-65)}$::GFP2 were detected in both the mitochondrial and peroxisomal fractions while GFP2 and $Cit2_{(1-8)}$::GFP2 were not. This result is consistent with that obtained for the high copy transformants of corresponding hybrid genes, except that a larger amount of organelle fraction was required for the development of visible positive signals. It is thus confirmable that overexpression of the fusion protein does not cause any distortion of the organelle targeting process directed by the N-terminal segment of Cit2p.

Lack of Dependence of Peroxisomal Import Mediated by the N-Terminal Segment of Cit2p on PEX5 and PEX7—In order to decipher whether the peroxisomal import process mediated by the N-terminal segment of Cit2p requires a novel peroxisomal import pathway, we analyzed the intracellular localization of GFP2 fusions containing varying lengths of Cit2p N-terminal sequences in *pex5* and *pex7* disrupants by confocal microscopy (Fig. 9). As expected, GFP2-SKL failed to be targeted into peroxisomes in the *pex5* disruptant (Fig. 9A_{1-4}), however, it was successfully imported into peroxisomes in the *pex7* disruptant (Fig. 9E_{1-4}). This result confirms that the C-terminal PTS1 of GFP2-SKL is recognized by Pex5p, the PTS1 receptor, but not by Pex7p, the PTS2 receptor. $Cit2_{(1-8)}$::GFP2 was not

Fig. 10. **Alignment of the *CIT1* and *CIT2* DNA sequences encoding the N-terminal parts of their products (*19*).** The start codons (ATG) of *CIT1* and *CIT2* are underlined, and gaps are indicated by dashes. Letters above and below the DNA sequences represent the amino acid sequences of Cit1p and Cit2p, respectively. The asterisked letters designate the first amino acid of the N-terminal amino acid sequence of the mature proteins (*22*).

Downloaded from http://jb.oxfordjournals.org/ at Peking University on October 1, 2012

imported into either mitochondria or peroxisomes, but was spread throughout the entire cytoplasm in both *pex5* (Fig. $9B_{1-4}$) and *pex7* disruptants (Fig. $9F_{1-4}$), as it was in the wild-type strain (*PEX5 PEX7*) (Fig. $6E_{1-4}$). In contrast, $Cit2_{(1-20)}$::GFP2 and $Cit2_{(1-65)}$::GFP2 were targeted to both mitochondria and peroxisomes, as well as being spread throughout the cytoplasm in both *pex5* (Fig. 9, C_{1-4} and D_{1-4}) and *pex7* mutants (Fig. 9, G_{1-4} and H_{1-4}). Therefore, in both *pex5* and *pex7* mutant strains, as in the wild-type strain, more than 8 N-terminal amino acids of Cit2p are required for the fusion proteins to be targeted to either organelle, and the first 20 amino acids of Cit2p are sufficient to constitute a cryptic ambidextrous targeting signal for both organelles. In addition, this result suggests that neither the *pex5* nor *pex7* mutation affects targeting behavior of the GFP derivatives containing the N-terminal segment of Cit2p and, accordingly, that the mitochondrial and peroxisomal targeting processes mediated by this segment do not require either Pex5p or Pex7p.

DISCUSSION

The peroxisomal citrate synthase (Cit2p) of *S. cerevisiae* terminates in SKL (*19*), while the mitochondrial form (Cit1p) begins with an N-terminal MTS and ends in SKN (*16*). Singh *et al.* (*34*) analyzed the importance of SKL as a topogenic signal for Cit2p and found that SKL is necessary for directing the protein to peroxisomes. They also showed that the C-terminal SKL is sufficient to target a leaderless version of Cit1p (that is, a version of the protein that lacks the N-terminal MTS) to peroxisomes, and that deletion of this tripeptide from the Cit2p protein causes the protein to be missorted to mitochondria. Furthermore, they also showed that a version of Cit2p that lacks both the C-terminal SKL and N-terminal 18 amino acids is not targeted into either organelle, suggesting that Cit2p contains a cryptic 18–amino acid N-terminal MTS.

We have found that the N-terminal 15 amino acids of Cit2p are cleaved during its import into peroxisomes despite the presence of a C-terminal PTS1 (*19*). In the current study, we analyzed the localization of the N-terminal domain–swapped citrate synthases and fusion proteins containing varying lengths of the Cit2p N-terminal sequence fused to GFP2, and found that an ambidextrous signal for both peroxisomes and mitochondria is included within the N-terminal 20 amino acids of Cit2p.

The results presented here lead to some additional points of discussion. First, our results show that Cit2p is a prime example of proteins that harbor more than one organelle targeting signal. Only a few proteins that carry a PTS1 are known to contain additional PTSs. Two examples of this phenomenon are *S. cerevisiae* Cta1p (*15*) and *H. polymorpha* peroxisomal matrix protein Per1p (*35*). Cta1p contains two independent signals, a C-terminal SSNSKF motif and the N-terminal third segment of the protein, which are sufficient but not necessary to target the protein to peroxisomes. Per1p contains both a carboxyl-terminal (PTS1) and an amino-terminal PTS (PTS2), both of which are capable of directing bacterial β-lactamase to the appropriate organelle.

Cit2p appears to contain a novel type of organelle targeting signal that is distinct from PTS2. Although devoid of the conserved PTS2 motif (RLXXXXXH/QL, in which X denotes any amino acid) (*6–8*, *13*), we demonstrated that the N-terminal sequence of Cit2p functions as a cryptic targeting signal for both mitochondria and peroxisomes. There are no other reports of such an N-terminal presequence that functions as an ambidextrous organelle targeting signal. One related report demonstrated that Pex7p (formerly Pas7p/Peb1p), a peroxisomal protein required for the import of thiolase into peroxisomes, is itself targeted to peroxisomes by its N-terminal 55 amino acids, which do not resemble PTS2 (*36*). A second interesting and related paper presented a mutational analysis of the N-terminal presequences (PTS2s) of rat peroxisomal 3-ketoacyl-CoA thiolase precursors. This study revealed that when the glutamate at position −11 (11 residues upstream from the cleavage site of the precursor protein) is changed to an amino acid other than aspartate, the signal peptide becomes effective in both peroxisomal and mitochondrial targeting (*37*).

We also found that the role of the N-terminal sequence of Cit2p as an ambidextrous targeting signal is minimized in the presence of the C-terminal SKL (PTS1), while the N-terminal MTS of Cit1p is equally functional with respect to PTS1. These observations suggest that the N-terminal sequence of Cit2p is considerably less efficient as an organelle targeting signal than are the MTS and PTS1. Thus, if the N-terminal sequence of Cit2p has its own receptor, the reduced efficiency of the N-terminal sequence in the presence of PTS1 might be caused by a low affinity of the signal for the receptor or a tightly restricted amount receptor.

We showed by immunoblotting that the molecular masses of the mature forms of $Cit2_{(1-20)}$::GFP2 found in the mitochondrial and peroxisomal fractions were smaller by ~2 kDa than those predicted from the corresponding ORF. Thus the N-terminal presequence (15 to 20 amino acids) of Cit2p appears to be cleaved as the protein is targeted to the organelle. This result is consistent with our previous suggestion that the 15 N-terminal amino acids of Cit2p are removed during its import into peroxisomes (*22*). While protein transport into mitochondria is normally accompanied by proteolytic cleavage of the N-terminal MTS, most peroxisomal proteins [such as *S. cerevisiae* thiolase (*6*)] are not subjected to any significant processing of the N-terminal signal upon peroxisomal import. There are a few peroxisomal proteins [such as mammalian (*10*) and plant (*8*) 3-ketoacyl-CoA-thiolases, and watermelon glyoxysomal malate dehydrogenase (*38*)] that possess a PTS2 and undergo N-terminal processing. However, even in the cases of peroxisomal proteins with cleavable PTS2 motifs, removal of the PTS2 is not thought to be an essential step in the import process. This is supported by the finding that in fibroblasts from some patients with peroxisome biogenesis disorders, the peroxisomal enzyme thiolase, although it is still imported into ghost peroxisomes, is present only in the immature precursor form (*39*, *40*). It is still unclear whether cleavage of the N-terminal sequence of Cit2p is indispensable for correct import into either peroxisomes or mitochondria. Thus further study of mutant fusion constructs with uncleavable N-terminal signals is needed.

In *S. cerevisiae*, two PTS receptors (Pex5p and Pex7p) have been identified. Pex5p, a hydrophilic 69-kDa protein containing eight tetratricopeptide repeats and no predicted membrane-spanning domains (*41*), has been shown to function as a cycling PTS1 receptor, and hence, to be involved the PTS1-specific branch of the peroxisomal import process

Downloaded from http://jb.oxfordjournals.org/ at Peking University on October 1, 2012

(*42, 43*). Pex7p, a 42-kDa hydrophilic protein has been found to be a PTS2 receptor and is essential to the PTS2-specific branch (*36, 44*). In addition to the PTS receptors, several peroxisomal membrane proteins that serve as receptor-docking proteins for the PTS receptors have been identified. Pex13p, a 43 kDa integral peroxisomal membrane protein, interacts directly with Pex5p, and hence, serves as a peroxisomal membrane receptor for at least one of the two peroxisomal signal recognition factors (*45*). Pex14p, another peroxisomal membrane protein, interacts with both the PTS1 and PTS2 receptors, as well as with two other membrane-bound peroxins including Pex13p (*46*). It is thus believed that there is a common translocation machinery for both PTS-dependent pathways in peroxisomal membranes. However, a receptor for the third type of PTS, the internal sequences such as those found in *C. tropicalis* acyl-CoA oxidase (*14*), has not yet been isolated and characterized. In this report, it is suggested that neither *pex5* nor *pex7* disruption affects the targeting behavior of GFP2 derivatives containing the N-terminal segment of Cit2p. These results imply that the mitochondrial and peroxisomal targeting process mediated by the N-terminal segment is not dependent on either Pex5p or Pex7p. This leads us to propose the existence of an additional branch in the peroxisomal import process that utilizes a novel receptor specific for the N-terminal segment of Cit2p. This receptor may also be involved in the mitochondrial import pathway.

Although the N-terminal signal of Cit2p is shown to have the capability to target proteins into both peroxisomes and mitochondria, we have not yet deciphered how Cit2p, which is destined for peroxisomes, came to have the N-terminal cryptic organelle targeting signal in addition to the C-terminal PTS1. A plausible explanation might be derived from the suggestion that one of the two citrate synthase genes of *S. cerevisiae* (*CIT1* and *CIT2*) arose by gene duplication of the other, followed by sequence divergence to create an MTS (if *CIT1* evolved from *CIT2*) or a PTS (if *CIT2* evolved from *CIT1*) (*19*). This suggestion is supported by the fact that the two proteins show a high degree of homology (81%) in their predicted amino acid sequences. In addition, *CIT1* and *CIT2* share several nucleotide stretches (up to eight nucleotides in length) with 100% matches distributed between codons 2 and 20 of *CIT1* and between nucleotide −75 (relative to the ATG) and the initiation codon of *CIT2*. The dramatic divergence in both their nucleotide and amino acid sequences is concentrated between codons 21 and 40 of *CIT1* and codons 2 and 21 of *CIT2*. Thus the N-terminal presequence of Cit2p may be present as a remnant of molecular evolution of the protein, rather than an essential element for peroxisomal import. More detailed functional analyses of the N-terminal presequence are needed before this issue can be resolved.

We wish to thank Drs. P. B. Lazarow and P. E. Purdue (Mount Sinai School of Medicine, New York, New York, USA) for yeast strains (W303a-1 and W303a-2), Dr. Bong-Kiun Kaang (Seoul National University, Seoul, Korea) for pNEXδ-S65T, and Mr. J.H. Lee and S.H. Nam for technical assistance.

REFERENCES

1. Douglas, M.G., McCammon, M., and Vassarotti, A. (1986) Targeting of proteins into mitochondria. *Microbiol. Rev.* **50**, 166–178
2. Glick, B.S., Beasley, E.M., and Schatz, G. (1992) Protein sorting in mitochondria. *Trends Biochem. Sci.* **17**, 453–459
3. Gould, S.J., Keller, G.A., Hosken, N., Wilkinson, J., and Subramani, S. (1989) A conserved tripeptide sorts proteins to peroxisomes. *J. Cell Biol.* **108**, 1657–1664
4. Miura, S., Oda, T., Funai, T., Ito, M., Okada, Y., and Ichiyama, A. (1994) Urate oxidase is imported into peroxisomes recognizing the C-terminal SKL motif of proteins. *Eur. J. Biochem.* **223**, 141–146
5. Miura, S., Kasuya-Arai, I., Mori, H., Miyazawa, S., Osumi, T., Hashimoto, T., and Fujiki, Y. (1992) Carboxyl-terminal consensus Ser-Lys-Leu-related tripeptide of peroxisomal proteins functions *in vitro* as a minimal peroxisome-targeting signal. *J. Biol. Chem.* **267**, 14405–14411
6. Glover, J.R., Andrews, D.W., Subramani, S., and Rachubinski, R.A. (1994) Mutagenesis of the amino targeting signal of *Saccharomyces cerevisiae* 3-ketoacyl-CoA thiolase reveals conserved amino acids required for import into peroxisomes *in vivo*. *J. Biol. Chem.* **269**, 7558–7563
7. Erdmann, R. (1994) The peroxisomal targeting signal of 3-oxoacyl-CoA thiolase from *Saccharomyces cerevisiae*. *Yeast* **10**, 935–944
8. Preisig-Muller, R. and Kindl, H. (1993) Thiolase mRNA translated *in vitro* yields a peptide with a putative N-terminal presequence. *Plant Mol. Biol.* **22**, 59–66
9. Hijikata, M., Wen, J.K., Osumi, T., and Hashimoto, T. (1990) Occurrence of 2 closely related but differentially regulated gene. *J. Biol. Chem.* **265**, 4600–4606
10. Swinkels, B.W., Gould, S.J., Bodnar, A.G., Rachubinski, R.A., and Subramani, S. (1991) A novel, cleavable peroxisomal targeting signal at the amino-terminus of the rat 3-ketoacyl-CoA thiolase. *EMBO J.* **10**, 3255–3262
11. Gietl, C. (1990) Glyoxysomal malate dehydrogenase from watermelon is synthesized with an amino-terminal transit peptide. *Proc. Natl. Acad. Sci. USA* **87**, 5773–5777
12. Faber, K.N., Haima, P., de Hoop, M.J., Harder, W., Veenhuis, M., and Ab, G. (1993) Peroxisomal amine oxidase of *Hansenula polymorpha* does not require its SRL-containing C-terminal sequence for targeting. *Yeast* **9**, 331–338
13. Faber, K.N., Keizer-Gunnink, I., Pluim, D., Harder, W., Ab, G., and Veenhuis, M. (1995) The N-terminus of amine oxidase of *Hansenula polymorpha* contains a peroxisomal targeting signal. *FEBS Lett.* **357**, 115–120
14. Small, G.M., Szabo, L.J., and Lazarow, P.B. (1988) Acyl-CoA oxidase contains two targeting sequences each of which can mediate protein import into peroxisomes. *EMBO J.* **7**, 1167–1173
15. Kragler, F., Langeder, A., Raupachova, J., Binder, M., and Hartig, A. (1993) Two independent peroxisomal targeting signals in catalase A of *Saccharomyces cerevisiae*. *J. Cell Biol.* **120**, 665–673
16. Suissa, M., Suda, K., and Schatz, G. (1984) Isolation of the nuclear yeast genes for citrate synthase and fifteen other mitochondrial proteins by a new screening method. *EMBO J.* **3**, 1773–1781
17. Kim, K.S., Rosenkrantz, M.S., and Guarente, L. (1986) *Saccharomyces cerevisiae* contains two functional citrate synthase genes. *Mol. Cell. Biol.* **6**, 1936–1942
18. Lewin, A.S., Hines, V., and Small, G.M. (1990) Citrate synthase encoded by the *CIT2* gene of *Saccharomyces cerevisiae* is peroxisomal. *Mol. Cell. Biol.* **10**, 1399–1405
19. Rosenkrantz, M., Alam, T., Kim, K.S., Clark, B.J., Srere, P.A., and Guarente, L.P. (1986) Mitochondrial and nonmitochondrial citrate synthase in *Saccharomyces cerevisiae* are encoded by distinct homologous genes. *Mol. Cell. Biol.* **6**, 4509–4515
20. Jia, Y.K., Becam, A.M., and Herbert, C.J. (1997) The *CIT3* gene of *Saccharomyces cerevisiae* encodes a second mitochondrial isoform of citrate synthase. *Mol. Microbiol.* **24**, 53–59
21. Cho, N.S., Kim, K.S., and Maeng, P.J. (1991) Purification and characterization of nonmitochondrial citrate synthase from *Saccharomyces cerevisiae*. *Kor. J. Microbiol.* **29**, 230–237
22. Lee, H.S., Choi, W.S., Lee, J.S., and Maeng, P.J. (1994) Organelle targeting of citrate synthases in *Saccharomyces cere-*

Downloaded from http://jb.oxfordjournals.org/ at Peking University on October 1, 2012

visiae. Kor. J. Microbiol. **32**, 558–564
23. Heim, R., Cubitt, A.B., and Tsien, R.Y. (1995) Improved green fluorescence [letter]. *Nature* **373**, 663–664
24. Ito, H., Fukuda, Y., Murata, K., and Kimura, A. (1983) Transformation of intact yeast cells treated with alkali cations. *J. Bacteriol.* **153**, 163–168
25. Hill, J.E., Myers, A.M., Koerner, T.J., and Tzagoloff, A. (1986) Yeast/*E. coli* shuttle vectors with multiple unique restriction sites. *Yeast* **2**, 163–167
26. Sambrook, J., Fritsch, E.F., and Maniatis, T. (1989) *Molecular Cloning: A Laboratory Manual*, Cold Spring Harbor Laboratory Press, Cold Spring Harbor, New York
27. Liao, X. and Butow, R.A. (1993) *RTG1* and *RTG2*: two yeast genes required for a novel path of communication from mitochondria to the nucleus. *Cell* **72**, 61–71
28. Gietz, R.D. and Sugino, A. (1988) New yeast-*Escherichia coli* shuttle vectors constructed with *in vitro* mutagenized yeast genes lacking six-base pair restriction sites. *Gene* **74**, 527–534
29. Kim, H.-K. and Kaang, B.-K. (1998) Truncated green fluorescent protein mutants and their expression in *Aplysia neurons*. *Brain Res. Bull.* **47**, 35–41
30. Cohen, G., Rapatz, W., and Ruis, H. (1988) Sequence of the *Saccharomyces cerevisiae CTA1* gene and amino acid sequence of catalase A derived from it. *Eur. J. Biochem.* **176**, 159–163
31. Srere, P.A. (1969) Citrate synthase. Methods Enzymol. **13**, 3–26.
32. Mason, T.L., Poyton, R.O., Wharton, D.C., and Schatz, G. (1973) Cytochrome c oxidase from baker's yeast: I. Isolation and Properties. *J. Biol. Chem.* **248**, 1346–1354
33. Baudhuin, P., Beaufay, H., Rahman-Li, Y., Sellinger, O.Z., Wattiaux, R., Jacques, P., and Duve, C.d. (1964) Tissue fractionation studies. 17. Intracellular distribution of monoamine oxidase, aspartate amino transferase, alanine aminotransferase, D-amino acid oxidase and catalase in rat liver tissue. *Biochem. J.* **92**, 179–184
34. Singh, K.K., Small, G.M., and Lewin, A.S. (1992) Alternative topogenic signals in peroxisomal citrate synthase of *Saccharomyces cerevisiae*. *Mol. Cell. Biol.* **12**, 5593–5599
35. Waterham, H.R., Titorenko, V.I., Haima, P., Cregg, J.M., Harder, W., and Veenhuis, M. (1994) The *Hansenula polymorpha PER1* gene is essential for peroxisome biogenesis and encodes a peroxisomal matrix protein with both carboxy- and amino-terminal targeting signals. *J. Cell Biol.* **127**, 737–749
36. Zhang, J.W. and Lazarow, P.B. (1996) Peb1p (Pas7p) is an intraperoxisomal receptor for the NH_2-terminal, type 2, peroxisomal targeting sequence of thiolase: Peb1p itself is targeted to peroxisomes by an NH_2-terminal peptide. *J. Cell Biol.* **132**, 325–334
37. Tsukamoto, T., Hata, S., Yokota, S., Miura, S., Fujiki, Y., Hijikata, M., Miyazawa, S., Hashimoto, T., and Osumi, T. (1994) Characterization of the signal peptide at the amino terminus of the rat peroxisomal 3-ketoacyl-CoA thiolase precursor. *J. Biol. Chem.* **269**, 6001–6010
38. Gietl, C., Faber, K.N., van der Klei, I.J., and Veenhuis, M. (1994) Mutational analysis of the N-terminal topogenic signal of watermelon glyoxysomal malate dehydrogenase using the heterologous host *Hansenula polymorpha*. *Proc. Natl. Acad. Sci. USA* **91**, 3151–3155
39. Balfe, A., Hoefler, G., Chen, W.W., and Watkins, P.A. (1990) Aberrant subcellular localization of peroxisomal 3-ketoacyl-CoA thiolase in the Zellweger syndrome and rhizomelic chondrodysplasia punctata. *Pediatr. Res.* **27**, 304–310
40. van Roermund, C.W., Brul, S., Tager, J.M., Schutgens, R.B., and Wanders, R.J. (1991) Acyl-CoA oxidase, peroxisomal thiolase and dihydroxyacetone phosphate acyltransferase: aberrant subcellular localization in Zellweger syndrome. *J. Inherit. Metab. Dis.* **14**, 152–164
41. Van der Leij, I., Franse, M.M., Elgersma, Y., Distel, B., and Tabak, H.F. (1993) *PAS10* is a tetratricopeptide-repeat protein that is essential for the import of most matrix proteins into peroxisomes of *Saccharomyces cerevisiae*. *Proc. Natl. Acad. Sci. USA* **90**, 11782–11786
42. Brocard, C., Kragler, F., Simon, M.M., Schuster, T., and Hartig, A. (1994) The tetratricopeptide repeat-domain of the *PAS10* protein of *Saccharomyces cerevisiae* is essential for binding the peroxisomal targeting signal-SKL. *Biochem. Biophys. Res. Commun.* **204**, 1016–1022
43. Dodt, G. and Gould, S.J. (1996) Multiple *PEX* genes are required for proper subcellular distribution and stability of Pex5p, the PTS1 receptor: evidence that PTS1 protein import is mediated by a cycling receptor. *J. Cell Biol.* **135**, 1763–1774
44. Rehling, P., Marzioch, M., Niesen, F., Wittke, E., Veenhuis, M., and Kunau, W.H. (1996) The import receptor for the peroxisomal targeting signal 2 (PTS2) in *Saccharomyces cerevisiae* is encoded by the *PAS7* gene. *EMBO J.* **15**, 2901–2913
45. Erdmann, R. and Blobel, G. (1996) Identification of Pex13p a peroxisomal membrane receptor for the PTS1 recognition factor. *J. Cell Biol.* **135**, 111–121
46. Albertini, M., Rehling, P., Erdmann, R., Girzalsky, W., Kiel, J.A., Veenhuis, M., and Kunau, W.H. (1997) Pex14p, a peroxisomal membrane protein binding both receptors of the two PTS-dependent import pathways. *Cell* **89**, 83–92

Downloaded from http://jb.oxfordjournals.org/ at Peking University on October 1, 2012